

## Title Page

# Gastrin-Releasing Peptide/Neuromedin B Receptor Antagonists, PD176252 and PD168368, and Related Analogs are Potent Agonists of Human Formyl-Peptide Receptors

Igor A Schepetkin, Liliya N. Kirpotina, Andrei I. Khlebnikov,

Mark A. Jutila, and Mark T. Quinn

*Department of Veterinary Molecular Biology, Montana State University, Bozeman, Montana (I.A.S., L.N.K., M.A.J., M.T.Q.) and Department of Chemistry, Altai State Technical University, Barnaul, Russia (A.I.K.)*

## Running Title Page

**Running title:** BB<sub>1</sub>/BB<sub>2</sub> Antagonists are Novel FPR Agonists

**Address for Correspondence:** Dr. Mark T. Quinn  
Veterinary Molecular Biology  
Montana State University  
Bozeman, MT 59717  
Phone: 406-994-5721; Fax 406-994-4303  
E-mail: mquinn@montana.edu

Number of text pages: 23

Number of tables: 6

Number of figures: 5

Number of references: 63 (58)

Number of words in Abstract: 238

Number of words in Introduction: 746 (640)

Number of words in Discussion: 1,715 (1,497)

## Abstract

N-formyl peptide receptors (FPRs) are G protein-coupled receptors (GPCR) involved in host defense and sensing cellular dysfunction. Thus, FPRs represent important therapeutic targets. In the present studies, we screened 32 ligands (agonists and antagonists) of unrelated GPCR for their ability to induce intracellular  $\text{Ca}^{2+}$  mobilization in human neutrophils and HL-60 cells transfected with human FPR1, FPR2, or FPR3. Screening of these compounds demonstrated that antagonists of gastrin-releasing peptide/neuromedin B receptors ( $\text{BB}_1/\text{BB}_2$ ), PD176252 and PD168368, were potent mixed FPR1/FPR2 agonists, with nanomolar  $\text{EC}_{50}$  values. Cholecystokinin-1 (CCK-1) receptor agonist A-71623 was also a mixed FPR1/FPR2 agonist, but with micromolar  $\text{EC}_{50}$  values. Screening of 56 Trp- and Phe-based PD176252/PD168368 analogs and 41 related non-peptide/non-peptoid analogs revealed 22 additional FPR agonists. Most were potent mixed FPR1/FPR2/FPR3 agonists with nanomolar  $\text{EC}_{50}$  for FPR2, making them among the most potent non-peptide FPR2 agonists reported to date. In addition, these agonists were also potent chemoattractants for murine and human neutrophils and activated reactive oxygen species production in human neutrophils. Molecular modeling of the selected agonists using field point methodology allowed us to modify our previously reported pharmacophore model for the FPR2 ligand binding site. This model suggests the existence of three hydrophobic/aromatic subpockets and several binding poses of FPR2 agonists in the transmembrane region of this receptor. These studies demonstrate that FPR agonists could include ligands of unrelated GPCR and that analysis of such compounds can enhance our understanding of pharmacological effects of these ligands.

## Introduction

*N*-formyl-methionyl-leucyl-phenylalanine (fMLF) is one of the most studied phagocyte chemoattractants and represents a prototype for microbe-derived formylated peptides (Schiffmann et al., 1975). Recent studies have shown that formylated peptides are also produced by mitochondria and can be released when mitochondria are damaged during tissue injury (Raoof et al., 2010). *N*-formyl peptides activate cells through formyl peptide receptors (FPRs), which are G protein-coupled receptors (GPCR) [reviewed in (Ye et al., 2009)]. The three human FPRs (FPR1, FPR2, and FPR3) are expressed on a variety of cell types, including neutrophils, macrophages, T lymphocytes, epithelial cells, hepatocytes, fibroblasts, astrocytes, and other cells that serve a variety of regulatory functions during the host defense response (review in (Ye et al., 2009; Gavins, 2010)). For example, FPR1 and FPR2 have been implicated in control of endogenous inflammatory processes and initiation of proinflammatory neutrophil responses to pathogenic bacteria (Kretschmer et al., 2010). The diverse tissue expression of these receptors suggests the possibility of as yet unappreciated complexity in the innate response and perhaps other unidentified functions for FPR family members. For example, mouse FPRs have been reported to be candidate chemosensory receptors in the vomeronasal organ (Liberles et al., 2009). Likewise, several studies have suggested that FPR2 agonists exhibit protective effects in ischemia–reperfusion models [reviewed in (Gavins, 2010)]. Overall, the demonstrated role of FPRs in orchestrating acute-phase inflammation supports the development of FPR agonists as novel anti-inflammatory therapeutics (Dufton and Perretti, 2010).

The conserved seven-transmembrane (7-TM) structure of GPCRs suggests the possibility that this superfamily may have evolved from a single ancestral protein (Fredriksson et al., 2003). Indeed, the common 7-TM structure and the presence of universally conserved residues in each of the TM helices make it possible to build rough models of the helical bundle for diverse

GPCRs (Katritch et al., 2010). Based on this structural conservation, privileged scaffolds can be selected that are able to provide high-affinity ligands for more than one type of receptor by targeting common conserved motifs of the GPCR superfamily (Parravicini et al., 2010). Indeed, such structural motifs have been successfully used to design and synthesize combinatorial libraries to probe for novel GPCR targets (Gloriam et al., 2009). Furthermore, it has been shown that various compounds can act as both agonists and/or antagonists for several GPCRs within the same or different subfamilies. For example, bile acids are antagonists of FPR1/FPR2 (Chen et al., 2000) and agonists for TGR5, a GPCR involved in regulating thyroid hormone signaling and energy homeostasis (Kawamata et al., 2003). Thus, it is reasonable that known GPCR ligands (agonists and/or antagonists) could be used in screening of unrelated GPCR targets to identify novel therapeutics.

To provide further insight in the specificity of different previously described GPCR ligands and identify novel and potentially higher affinity FPR agonists, we screened 32 relatively low-molecular weight ligands (agonists and antagonists) of 24 unrelated GPCRs using a  $\text{Ca}^{2+}$  mobilization assay in human neutrophils and HL-60 cells transfected with human FPR1, FPR2, or FPR3. Interestingly, we found that two bombesin-related  $\text{BB}_1/\text{BB}_2$  antagonists, PD176252 and PD168368, were potent mixed type FPR agonists, with  $\text{EC}_{50}$  values in the nanomolar range. After further structure–activity relationship (SAR) analysis and analog screening, we identified 22 additional mixed type FPR agonists with  $\text{EC}_{50}$  values in the low micromolar and nanomolar ranges. In addition, these agonists were also potent chemoattractants for murine and human neutrophils and activated reactive oxygen species (ROS) production in human neutrophils. Molecular modeling of selected FPR agonists using the field point methodology allowed us to modify our previously reported pharmacophore model (Kirpotina et al., 2010) for the ligand binding site of FPR2. These studies demonstrate for the first time that selected bombesin

receptor BB<sub>1</sub>/BB<sub>2</sub> antagonists, PD176252 and PD168368, their Trp- and Phe-based derivatives, and related non-peptoid/non-peptide analogs are potent FPR agonists and that analysis of such compounds can enhance our understanding of ligand–FPR interactions.

## Materials and Methods

**Materials.** 8-Amino-5-chloro-7-phenylpyridol[3,4-*d*]pyridazine-1,4(2*H*,3*H*)-dione (L-012) was obtained from Wako Chemicals (Richmond, VA). Dimethyl sulfoxide (DMSO), horseradish peroxidase (HRP), *N*-formyl-Met-Leu-Phe (fMLF), and Histopaque 1077 were purchased from Sigma Chemical Co. (St. Louis, MO). Peptides Trp-Lys-Tyr-Met-Val-D-Met (WKYMVm) and Trp-Lys-Tyr-Met-Val-L-Met (WKYMVM) were from Calbiochem (San Diego, CA) and Tocris Bioscience (Ellisville, MO), respectively. Tetramethylbenzidine (TMB) was from BD Bioscience Pharmingen (San Diego, Ca). RPMI-1640 medium without phenol red was from Lonza (Walkersville, MD). Hanks' balanced salt solution (HBSS; 0.137 M NaCl, 5.4 mM KCl, 0.25 mM Na<sub>2</sub>HPO<sub>4</sub>, 0.44 mM KH<sub>2</sub>PO<sub>4</sub>, 4.2 mM NaHCO<sub>3</sub>, 5.56 mM glucose, and 10 mM HEPES, pH 7.4) was from Invitrogen (Carlsbad, CA). HBSS containing 1.3 mM CaCl<sub>2</sub> and 1.0 mM MgSO<sub>4</sub> is designated as HBSS<sup>+</sup>. Percoll stock solution was prepared by mixing Percoll with 10× HBSS at a ratio of 9:1.

Screening compounds were purchased from Tocris Bioscience (Ellisville, MO), ChemBridge (San Diego, CA), InterBioScreen (Moscow, Russia), Albany Molecular Research (Albany, NY), and ChemDiv (San Diego, CA). The purity and identity of the compounds were verified using NMR spectroscopy, elemental analysis, and mass spectroscopy, as performed by the suppliers. The compounds were diluted in DMSO at a concentration of 20 mM and stored at −20°C.

**Cell Culture.** Human promyelocytic leukemia HL-60 cells stably transfected with human FPR1, FPR2, or FPR3 were cultured in RPMI-1640 supplemented with 10% heat-inactivated fetal calf serum, 10 mM HEPES, 100 µg/ml streptomycin, 100 U/ml penicillin, and G418 (1 mg/ml), as described previously (Christophe et al., 2002). Wild-type HL-60 cells were cultured under the same conditions, but without G418.

**Neutrophil Isolation.** For isolation of human neutrophils, blood was collected from healthy donors in accordance with a protocol approved by the Institutional Review Board at Montana State University. Neutrophils were purified from the blood using dextran sedimentation, followed by Histopaque 1077 gradient separation and hypotonic lysis of red blood cells, as described previously (Schepetkin et al., 2007). Isolated neutrophils were washed twice and resuspended in HBSS. Neutrophil preparations were routinely >95% pure, as determined by light microscopy, and >98% viable, as determined by trypan blue exclusion.

For murine neutrophil isolation, bone marrow leukocytes were flushed from tibias and femurs of BALB/c mice with HBSS, filtered through a 70- $\mu$ m nylon cell strainer (BD Biosciences, Franklin Lakes, NJ) to remove cell clumps and bone particles, and resuspended in HBSS at  $1 \times 10^6$  cells/ml. Bone marrow neutrophils were isolated from bone marrow leukocyte preparations, as described previously (Schepetkin et al., 2007). Briefly, bone marrow leukocytes were resuspended in 3 ml of 45% Percoll solution and layered on top of a Percoll gradient consisting of 2 ml each of 50, 55, 62, and 81% Percoll solutions in a conical 15-ml polypropylene tube. The gradient was centrifuged at 1600g for 30 min at 10°C, and the cell band located between the 61 and 81% Percoll layers was collected. The cells were washed, layered on top of 3 ml of Histopaque 1119, and centrifuged at 1600g for 30 min at 10°C to remove contaminating red blood cells. The purified neutrophils were collected, washed, and resuspended in HBSS. All animal use was conducted in accordance with a protocol approved by the Institutional Animal Care and Use Committee at Montana State University.

**Ca<sup>2+</sup> Mobilization Assay.** Changes in intracellular Ca<sup>2+</sup> were measured with a FlexStation II scanning fluorometer using fluorescent dye Fluo-4AM (Invitrogen) for human and murine neutrophils and HL-60 cells. All active compounds were evaluated in wild-type HL-60 cells to verify that the agonists were inactive in non-transfected cells. Neutrophils or HL-60



cells, suspended in HBSS, were loaded with Fluo-4AM dye (1.25  $\mu\text{g/ml}$  final concentration) and incubated for 30 min in the dark at 37°C. After dye loading, the cells were washed with HBSS, resuspended in HBSS<sup>+</sup>, and aliquotted into the wells of flat-bottom, half-area-well black microtiter plates (2 x 10<sup>5</sup> cells/well). The compound source plate contained dilutions of test compounds in HBSS<sup>+</sup>. Changes in fluorescence were monitored ( $\lambda_{\text{ex}}$  = 485 nm,  $\lambda_{\text{em}}$  = 538 nm) every 5 s for 240 s at room temperature after automated addition of compounds. Maximum change in fluorescence, expressed in arbitrary units over baseline, was used to determine agonist response. Responses were normalized to the response induced by 5 nM fMLF for HL-60 FPR1 and neutrophils or 5 nM WKYMVm for HL-60 FPR2 and HL-60 FPR3 cells, which were assigned a value of 100%. Curve fitting (at least 5-6 points) and calculation of median effective concentration values (EC<sub>50</sub>) were performed by nonlinear regression analysis of the dose–response curves generated using Prism 5 (GraphPad Software, Inc., San Diego, CA).

**Degranulation Assay.** Degranulation of azurophil granules was determined by measuring release of myeloperoxidase (MPO), as previously described (Zhang et al., 2007b). Human neutrophils (5 x 10<sup>6</sup> cells/ml in RPMI-1640) were treated with test compounds, fMLF, or DMSO, incubated for 30 min at 37°C, and centrifuged at 550g for 3 min. Aliquots of the supernatants (100  $\mu\text{l}$ ) were mixed with 100  $\mu\text{l}$  TMB in a 96-well flat-bottom transparent microtiter plate and incubated at room temperature for 15 min. The reaction was terminated by addition of 50  $\mu\text{l}$  5% phosphoric acid, and the absorbance was read at 450 nm in a SpectraMax Plus microtiter plate reader (Molecular Devices, Sunnyvale, CA).

**Chemotaxis Assay.** Human or murine neutrophils were suspended in HBSS<sup>+</sup> containing 2% (v/v) heat inactivated fetal bovine serum (FBS) (2 x 10<sup>6</sup> cells/ml), and chemotaxis was analyzed in 96-well ChemoTx chemotaxis chambers (Neuroprobe, Gaithersburg, MD), as described previously (Schepetkin et al., 2007). In brief, lower wells were loaded with 30  $\mu\text{l}$  of

HBSS<sup>+</sup> containing 2% (v/v) FBS and the indicated concentrations of test compounds, DMSO (negative control), or 1 nM fMLF as a positive control. Neutrophils were added to the upper wells and allowed to migrate through the 5.0- $\mu$ m pore polycarbonate membrane filter for 60 min at 37°C and 5% CO<sub>2</sub>. The number of migrated cells was determined by measuring ATP in lysates of transmigrated cells using a luminescence-based assay (CellTiter-Glo; Promega, Madison, WI), and luminescence measurements were converted to absolute cell numbers by comparison of the values with standard curves obtained with known numbers of neutrophils. Curve fitting (at least 8-9 points) and calculation of median effective concentration values (EC<sub>50</sub>) were performed by nonlinear regression analysis of the dose-response curves generated using Prism 5.

**Analysis of ROS Production.** ROS production was determined by monitoring L-012-enhanced chemiluminescence, which represents a sensitive and reliable method for detecting ROS production (Daiber et al., 2004). Human neutrophils were resuspended at 5 x 10<sup>5</sup> cells/mL in HBSS<sup>+</sup> and supplemented with 40  $\mu$ M L-012 and 8  $\mu$ g/ml HRP. Cells (100  $\mu$ l) were aliquoted into wells of 96-well flat-bottom white microtiter plates containing test compounds diluted in 100  $\mu$ l HBSS<sup>+</sup> (final DMSO concentration of 0.5%). Changes in luminescence were monitored every 5 s for 120 s at room temperature using a Fluroscan Ascent FL microtiter plate reader (Thermo Electron, Waltham, MA). The curve of light intensity (in relative luminescence units) was plotted against time, and the area under the curve was calculated as total luminescence. Curve fitting (at least 5-6 points) and calculation of median effective concentration values (EC<sub>50</sub>) were performed by nonlinear regression analysis of the dose-response curves generated using Prism 5 (GraphPad Software, Inc., San Diego, CA).

**Molecular Modeling.** Five agonists with known enantiomeric configurations and relatively high activity at FPR2 were chosen for pharmacophore modeling. The selected

structures included PD168368, AG-10/5, AG-10/8, AG-10/17, and compound **11** from (Frohn et al., 2007) (designated here as Frohn-11). We used a ligand-based approach for molecular modeling based on the use of field points (Cheeseright et al., 2007), as described in our previous studies (Kirpotina et al., 2010). The structures of the compounds in Tripos MOL2 format were imported into the FieldTemplater program (FieldTemplater Version 2.0.1; Cresset Biomolecular Discovery Ltd., Hertfordshire, UK). The conformation hunter algorithm was used to generate representative sets of conformations corresponding to local minima of energy calculated within the extended electron distribution (XED) force field (Vinter, 1994; Cheeseright et al., 2007). This algorithm incorporated in the FieldTemplater and FieldAlign software allowed us to obtain up to 200 independent conformations, which were passed to further calculation of field points surrounding each conformation of each molecule. To decrease the number of rotatable bonds during the conformation search, the “force amides trans” option was enabled in the program. For the generation of field point patterns, probe atoms having positive, negative, and zero charge were placed in the vicinity of a given conformation, and the energy of their interaction with the molecular field was calculated using the extended electron distribution parameter set. Positions of energy extrema for positive probes give “negative” field points, whereas energy extrema for negative and neutral probe atoms correspond to “positive” and steric field points, respectively. Hydrophobic field points were also generated with neutral probes capable of penetrating into the molecular core and reaching extrema in the centers of hydrophobic regions (e.g., benzene rings). The size of a field point depends on magnitude of an extremum (Cheeseright et al., 2006). There are approximately the same number of field points as heavy atoms in a “drug-like” molecule, and the field points are colored according to the following convention: blue, electron-rich (negative); red, electron-deficient (positive); yellow, van der Waals attractive (steric); and orange, hydrophobic (Cheeseright et al., 2007). A detailed description of the field point calculation

procedure has been published elsewhere (Cheeseright et al., 2006). A clique matching algorithm with further simplex optimization was applied to obtain the conformations of five molecules giving good mutual overlays in terms of geometric and field similarity. The best overlay was taken as a template representative of the bioactive conformation.

Additional specific FPR2 agonists, including compound **25** (designated here as Bürli-25) (Bürli et al., 2006), compound **14x** (designated here as Cilibrizzi-14x) (Cilibrizzi et al., 2009), AG-09/3, AG-09/4, AG-09/5, AG-09/6, AG-09/8, and AG-09/42 and mixed type FPR1/FPR2 agonists AG-09/9, AG-09/10 (Kirpotina et al., 2010) were superimposed onto the template using the FieldAlign program (FieldAlign Version 2.0.1; Cresset Biomolecular Discovery Ltd., Hertfordshire, UK). The molecular structures were imported into FieldAlign in Tripos MOL2 format. Conformational search and field point calculation were performed as described above for template building. Conformations with the best fit to the geometry and field points of the template were identified, and their superimpositions were refined by the simplex optimization algorithm incorporated in FieldAlign.

## Results

**Identification of FPR Agonists by Screening of Known GPCR Ligands.** The subset of 32 ligands was selected from the parent library of 100 different GPCR ligands as compounds that contained at least two heterocycles separated by a chemical linker with >2 bonds, because previous studies have shown that these characteristics are almost always present in low-molecular weight synthetic FPR1/FPR2 agonists (Nanamori et al., 2004; Edwards et al., 2005; Bürli et al., 2006; Frohn et al., 2007; Schepetkin et al., 2007; Schepetkin et al., 2008; Kirpotina et al., 2010). The selected 32 compounds represented ligands of 24 different GPCR, including a nociceptin receptor agonist (NNC 63-0532), three CCK-1 receptor antagonists (devazepide, A-71623, and SR 27897), two CCK-2 receptor antagonists (YM 022 and LY 288513), three cannabinoid CB<sub>2</sub> receptor ligands (BML-190, AM 630, and GW 405833), a neuropeptide Y<sub>5</sub> receptor antagonist (S 25585), two thyrotropin receptor agonists (taltirelin and NCGC00168126-01), a vasopressin 1A receptor antagonist (SR 49059), a protease-activated receptor 2 agonist (AC 55541), a sphingosine-1-phosphate receptor antagonist (JTE 013), a neuropeptide FF receptor antagonist (RF9), a neurotensin receptor antagonist (SR 142948), an endothelin A receptor antagonist (FR 139317), a cysteinyl leukotriene receptor 1 antagonist (ONO 1078), a growth hormone secretagogue receptor 1a agonist (L-692,585), a gonadotropin-releasing hormone receptor antagonist (T 98475), an oxytocin receptor antagonist (L-371,257), three tachykinin NK<sub>1</sub> receptor antagonists (FK 888, SDZ NKT 343, and L-732,138), a platelet-activating factor receptor antagonist (WEB 2086), a prostanoid EP<sub>4</sub> receptor antagonist (L-161,982), a serotonin 5-HT<sub>4</sub> receptor agonist (cisapride), a somatostatin sst<sub>2</sub> receptor agonist (L-054,264), a melanocortin 4 (MC<sub>4</sub>) receptor agonist (THIQ), and two BB<sub>1</sub>/BB<sub>2</sub> antagonists (PD168368 and PD176252).

Screening of the 32 GPCR ligands for their ability to induce  $\text{Ca}^{2+}$  mobilization in human neutrophils demonstrated that three such compounds were indeed neutrophil agonists. Structures of the active compounds and representative kinetic curves for  $\text{Ca}^{2+}$  mobilization in human neutrophils are shown in Figure 1, and activities of the compounds are reported in Table 1. The CCK-1 receptor agonist A-71623 (Boc-Trp-Lys( $\epsilon$ -N-2-methylphenylaminocarbonyl)-Asp-(N-methyl)-Phe-NH<sub>2</sub>) (Sugg et al., 1995) exhibited modest activity, with an EC<sub>50</sub> of ~18.3  $\mu\text{M}$ . In contrast, the bombesin-related BB<sub>1</sub>/BB<sub>2</sub> antagonists, PD168368 ((S)-a-methyl-a-[[[(4-nitrophenyl)amino]carbonyl]amino]-N-[[1-(2-pyridinyl) cyclohexyl]methyl]-1H-indole-3-propanamide) (Ryan et al., 1999) and PD176252 ((S)-N-[[1-(5-methoxy-2-pyridinyl)cyclohexyl]methyl]-a-methyl-a-[-(4-nitrophenyl)amino] carbonyl]amino-1H-indole-3-propanamide) (Ashwood et al., 1998) were highly active and stimulated [ $\text{Ca}^{2+}$ ]<sub>i</sub> release in human neutrophils with EC<sub>50</sub> values in the nanomolar range. Additionally, PD168368 and PD176252 stimulated degranulation of neutrophil azurophil granules (i.e., release of MPO), which was comparable to that induced by fMLF (Figure 1C). In contrast, A-71623 did not induce azurophil degranulation over the concentration range tested, indicating it may activate a different array of responses than PD168368/PD176252.

Specificity of the selected neutrophil agonists was verified by their ability to activate  $\text{Ca}^{2+}$  mobilization in HL-60 cells transfected with human FPRs, and we found A-71623 and PD176252 to be mixed FPR1/FPR2 agonists, while PD168368 was a mixed FPR1/FPR2/FPR3 agonist (Table 1). PD176252 and PD168368 had very high efficacy, inducing responses similar in amplitude to those induced by fMLF or WKYMVm, whereas A-71623 had somewhat lower efficacy. No response was observed in control, untransfected HL-60 cells treated with these compounds. The activities of PD176252 and PD168368 in HL-60 FPR2 cells were higher than or comparable to previously reported non-peptide FPR2 agonists, such as Quin-C1 (EC<sub>50</sub>=1.4

$\mu\text{M}$ ) (Nanamori et al., 2004) and AG-09/42 ( $\text{EC}_{50}=0.1 \mu\text{M}$ ) (Kirpotina et al., 2010), or synthetic peptides, such as HFYLP and its analogs (Bae et al., 2003a). Thus, our data demonstrate that the CCK-1 receptor agonist A-71623 and the bombesin-related  $\text{BB}_1/\text{BB}_2$  antagonists PD168368 and PD176252 can interact with GPCR unrelated to CCK-1 and  $\text{BB}_1/\text{BB}_2$ , respectively.

Since PD168368 and PD176252 were the most potent FPR agonists from our screen, we focused further efforts on investigation these compounds and their analogs. To determine whether other bombesin-related receptor ligands activated  $\text{Ca}^{2+}$  mobilization in human neutrophils and FPR-transfected HL-60 cells, we evaluated nine other commercially available  $\text{BB}_1/\text{BB}_2$  ligands, including three agonists [BIM 187, bombesin, and gastrin-releasing peptide (GRP)] and six antagonists (BIM 189, BIM 23042, BIM 23127, [D-Phe<sup>12</sup>]-bombesin, [D-Phe<sup>12</sup>,Leu<sup>14</sup>]-bombesin, and ICI 216,140). None of these ligands was found to activate neutrophil  $\text{Ca}^{2+}$  mobilization when tested over a concentration range of 1-50  $\mu\text{M}$ , and these ligands (at concentrations 1 and 10  $\mu\text{M}$ ) did not desensitize WKYMVm-induced  $\text{Ca}^{2+}$  mobilization in human neutrophils (data not shown). Thus, our results suggest that FPR agonist activity is due to specific structural features of PD168368 and PD176252 and not a general effect of all  $\text{BB}_1/\text{BB}_2$  ligands. In addition, these data support the conclusion that PD168368 and PD176252 are true FPR ligands and are not stimulating cells through bombesin receptors.

### Identification of Additional FPR Agonists by Screening PD168368/PD176252

**Analogs.** The  $\text{BB}_1/\text{BB}_2$  antagonists, PD168368 and PD176252, are characterized by a peptid scaffold, but also include an N-phenylurea substructure on one end of the molecule (see Figure 1A). Previously, we found that N-phenethyl-N'-phenylurea derivatives activated neutrophil functional responses and included FPR2-specific agonists (Schepetkin et al., 2008; Kirpotina et al., 2010). Likewise, Bürli et al. (Bürli et al., 2006) identified potent and specific FPR2 agonists with a 1-(3-oxo-2-phenyl-2,3-dihydro-1H-pyrazol-4-yl)-3-phenylurea scaffold. Since aromatic

amino acids (Trp, Phe, and Tyr) of peptide FPR1/FPR2 agonists have also been shown to be important moieties for ligand–receptor interactions (Bae et al., 2003b;Bae et al., 2004;Cavicchioni et al., 2006;Wan et al., 2007;Movitz et al., 2010), we selected Trp- and Phe-based N-phenylurea derivatives and related analogs for further screening. These 97 compounds included 7 Trp-based, 49 Phe-based, and 41 other non-peptoid derivatives (see Tables 2-4 and Supplemental Table S1 for structural details).

Compounds that induced  $\text{Ca}^{2+}$  mobilization in human neutrophils and HL-60 cells transfected with FPR1, FPR2, or FPR3 are shown in Tables 2-4 (chemical names for most potent compounds are indicated in the Table 5 legend), whereas non-active compounds are listed in Supplemental Table 1S. Non-active compounds induced no  $\text{Ca}^{2+}$  flux or had very low efficacy (<25% of positive control peptide) in human neutrophils. Our screening demonstrated that 3 Trp-based analogs, 10 Phe-based analogs, and 9 other analogs were agonists for human neutrophils and FPR-transfected HL-60 cells. In general, the active analogs also exhibited high efficacy, although a couple exceptions were present (see Tables 2-4). Among the most potent in human neutrophils, compounds AG-10/16 and AG-10/22 had  $\text{EC}_{50}$  values in the low nanomolar range ( $\text{EC}_{50}$  ~60 and 13 nM, respectively) and very high efficacy (>100%). When evaluated in HL-60 cells, most of the 22 compounds were mixed FPR1/FPR2 agonists, although many displayed much higher selectivity for either FPR1 or FPR2, as demonstrated by comparing the  $\text{EC}_{50}$  values at FPR1 to  $\text{EC}_{50}$  values at FPR2 for each agonist (see Tables 2-4). Twenty-one compounds had nanomolar  $\text{EC}_{50}$  values in FPR2-HL-60 cells and 4 compounds had nanomolar  $\text{EC}_{50}$  values in FPR1-HL-60 cells (Tables 2-4). Sixteen compounds were also active in FPR3-HL-60 cells, with AG-10/8 and AG-10/22 being the most potent (Tables 2-4). N-[1,3-di(benzodioxolan-5-yl)propan-2-yl]-N'-phenylurea and N-[2-(1,3-benzodioxol-5-yl)-1-benzylethyl]-N'-phenylurea derivatives displayed the highest selectivity for FPR2 *versus* FPR1



or FPR3 (Table 4), and AG-10/22 had the highest activity at FPR2 among all agonists identified ( $EC_{50} \sim 200$  pM with  $>100\%$  efficacy). In any case, further SAR analysis and biological studies will be needed to determine a role of different substituents in the receptor selectivity of related FPR agonists.

**Effect of Active Compounds on Neutrophil Functional Responses.** Compounds that activated  $Ca^{2+}$  mobilization in human neutrophils and transfected HL-60 cells also activated  $Ca^{2+}$  flux in murine neutrophils (Table 5). As with human neutrophils, AG-10/22 was the most potent agonist for murine neutrophils ( $EC_{50} \sim 3$  nM). The selected compounds were also chemoattractants for murine and human neutrophils (Table 5), and representative bell-shaped dose response curves are shown in Figure 2 for human neutrophil chemotactic responses. Similar response curves were found with murine neutrophils (data not shown). The most potent chemotactic compounds for murine and human neutrophils were AG-10/10 and AG-10/22, respectively.

FPR agonists identified in the  $Ca^{2+}$  mobilization screening were evaluated for their ability to activate human neutrophil ROS production in comparison with chemoattractant peptides fMLF and WKYMVm. Both peptides induced ROS production with a very similar time course and a peak of activity at  $\sim 1$  min (Figure 3A), which is comparable to previous reports (Karlsson et al., 2006; Thoren et al., 2010). Analysis of the ability of selected FPR agonists (Table 5) to activate ROS production in human neutrophils showed that these compounds stimulated ROS production with kinetic curves similar to the chemoattractant peptides, but with a lower amplitude. As an example, kinetics of ROS production is shown for AG-10/22 in Figure 3A. We found that most of the lead FPR agonists dose-dependently stimulated ROS production, with  $EC_{50}$  values in the nanomolar or low micromolar ranges (Figure 3B, Table 5). Interestingly,

PD168368 and PD176252 were classified as non-active compounds for stimulating ROS production, as their efficacy was <30% of background level.

We also examined whether fMLF, WKYMVm, or WKYMVM pretreatment desensitized the neutrophil response to selected compounds, including PD168368, AG-10/5, AG-10/8, AG-10/16, and AG-10/22, and *vice versa*. We found that pretreatment with the selected compounds (or peptides) markedly attenuated  $\text{Ca}^{2+}$  mobilization induced by the peptides or selected compounds, respectively. As examples, kinetic traces of  $\text{Ca}^{2+}$  flux are shown for PD168368 and AG-10/16 in Figure 4. These data further demonstrate that the selected compounds are FPR agonists and can desensitize FPR to subsequent stimulation.

**Structure–Activity Relationship Analysis of Selected FPR Agonists.** The active FPR agonists with Trp/Phe-based scaffolds contained a variety of  $\text{R}_2$  substituents, which ranged from a relatively small N-pyrrolidine (AG-10/4) to a bulky 6,7-dimethoxy-1,2,3,4-tetrahydroisoquinoline (AG-10/13). Note, however, that modification of the  $\text{R}_2$  substituent did affect agonist selectivity and/or potency. For example, comparison of our previously reported N-phenethyl-N'-phenylurea FPR2-specific agonists (Kirpotina et al., 2010) with the Trp/Phe-based FPR agonists and their related analogs identified here demonstrated that introduction of additional heterocycle-containing groups to the carbon atom in the  $\alpha$ -position to the carbamide fragment increased potency at FPR2, but led to loss of specificity. Likewise, introduction of an ethyl acetate group into the *meta* position of the N-piperidine ring increased agonist activity (compare AG-10/5 and AG-10/9), but shifting of the ethyl acetate group from the *meta* to the *para* position resulted in decrease FPR2 activity and loss of FPR1 and FPR3 activity (compare AG-10/9 and AG-10/10).

Most potent agonists with  $\text{EC}_{50}$  values in the nanomolar range contained a halogen atom in the *para*-position of the N'-phenylurea moiety. While the presence of the halogen atom was

not absolutely essential for FPR activity, its absence did result in decreased activity. For example, substitution of *para*-Br or *para*-Cl with an S-Me group (compare AG-10/5 or AG-10/6 and AG-10/7) or a Me group (compare AG-10/16 or AG-10/17 and AG-10/18) led to decreased activity in human neutrophils and FPR-transfected HL-60 cells. In addition, moving the halogen atom from the *para* position to the *meta* (AG-10/76 and AG-10/95) or *ortho* (AG-10/83 and AG-10/89) positions resulted in complete loss of activity at all FPRs. This finding is similar to previous studies showing that shift of a halogen atom in the phenyl group of the N'-phenylurea moiety from the *para* position to the *meta* or *ortho* positions resulted in loss of FPR agonist activity (Bürli et al., 2006; Kirpotina et al., 2010).

All active FPR agonists (Tables 2-4) were S-enantiomers or racemic mixtures of R- and S-enantiomers. We did not have pairs of compounds with distinct enantiomeric configurations in our synthetic library, and further synthesis and analysis will be needed to verify whether a specific configuration is preferred for any given molecule.

**Pharmacophore Modeling of Ligand Recognition.** Previously, we applied a ligand-based approach to molecular modeling of FPR2 (Kirpotina et al., 2010) that used field point methodology (Cheeseright et al., 2006; Cheeseright et al., 2007). To revise and expand this model, we selected five agonists with known enantiomeric configurations, different heterocyclic fragments, and relatively high selectivity for FPR2 in comparison with FPR1/FPR3 (>100-fold more active for FPR2, making them essentially specific for FPR2). In comparison with previously described FPR2 agonists (Kirpotina et al., 2010), these compounds bear additional heterocycle-containing groups at the carbon atom in the  $\alpha$ -position to the carbamide fragment (see Tables 2-3). The selected agonists included: PD168368, AG-10/5, AG-10/8, AG-10/17, and Frohn-11 (Frohn et al., 2007). This chiral compound was used to increase diversity of scaffolds used for building the template.

Using the conformer hunt algorithm (FieldTemplater Version 2.0.1), we generated up to 200 independent conformations lying within 6-kcal/mol energy gap above the lowest-energy geometry for each of the molecules. Field point patterns were calculated for these conformations, and the clique algorithm of FieldTemplater was applied to obtain the best alignment for this group of 5 agonists. Analysis of all conformations of the five compounds led to the construction of three 5-molecule templates very similar to each other in molecular geometry and quality of overlays, providing evidence that a stable solution was obtained by the FieldTemplater program. The best template shown in Figure 5A was taken for further investigation. A schematic representation of the template and three hypothetical hydrophobic subpockets are shown in Figure 7. Furthermore, relative locations of substituents inside the different subpockets are indicated in Table 6.

One of the notable features of the template is the good overlap of phenylurea fragments in compounds PD168368, AG-10/5, AG-10/8, and AG-10/17. Electron-withdrawing substituents in the *para*-position of phenyl ring produce a group of blue points where an electropositive area of the receptor could be located. In the centers of the superimposed phenylurea benzene rings, orange field points reflect the hydrophobic nature of the benzene fragments (Figure 5A). Thus, it is reasonable to suggest the presence of a hydrophobic pocket (subpocket I) with positively charged groups in the binding site of FPR2. Another pocket with hydrophobic character (subpocket II) corresponds to the overlapping benzyl substituents of molecules AG-10/5 and AG-10/8. This location also coincides with the fused benzene rings of indole, benzodioxolane, and benzimidazole fragments in compounds PD168368, AG-10/17, and Frohn-11, respectively. An additional subpocket III of the proposed FPR2 agonist-binding site is occupied by piperidine, azepinone, and (2-pyridyl)cyclohexyl groups of molecules AG-10/5, AG-10/8, and PD168368, as well as by the second benzodioxolane heterocycle of AG-10/17.

Although hydrophobic points dominate in the center of this area, one being produced by the ethyl side chain of Frohn-11, a cloud of blue and red field points is present in the vicinity of subpocket III. These points may correspond to groups responsible for hydrogen bonding and/or electrostatic interactions between the receptor and ligand heteroatoms. Finally, noticeable groups of blue and red field points are seen near the overlapping carbonyl and NH groups, respectively (Figure 5A). It is very likely that corresponding areas of the receptor participate in hydrogen bond formation with ligands.

Additional specific FPR2 agonists Bürli-25, Cilibrizzi-14x, AG-09/3, AG-09/4, AG-09/5, AG-09/6, AG-09/8, AG-09/9, and mixed FPR1/FPR2 agonists AG-09/10, and AG-09/42 were overlaid on the 5-molecule template of FPR2. The main steps, namely conformational searches, field point generation, finding preliminary overlays by clique matching and their subsequent simplex optimization were performed by built-in modules of FieldAlign software (see Methods). It should be noted that conformations of the same molecule produce various overlays onto the template which differ in similarity score. The highest-score superimpositions are shown in Table 6. As examples, overlaid molecules occupying subpockets I and II (AG-09/42) or subpockets I and III (Cilibrizzi-14x) are shown in Figure 5B. The above-mentioned modes of superimposition were found for at least three overlays with high similarity scores for each molecule.

A reasonable way to analyze the results obtained is to identify which of the fragments of overlaid molecules occupies each of the three subpockets (Table 6). Subpocket I is always occupied by the terminal phenyl ring of N-phenylurea (N-phenylthiourea) or N-phenylamide (Bürli-25, Cilibrizzi-14x, AG-09/1, AG-09/3, AG-09/4, AG-09/6, AG-09/9, AG-09/10, and AG-09/42). For AG-09/5 and AG-09/8, the benzene ring of a substituted benzoyl is located in subpocket I (Figure 7B). Most FPR agonists overlaid in a two-subpocket mode. In addition to subpocket I, the second occupied region was either subpocket II (AG-09/1, AG-09/3, AG-09/4,

AG-09/6, and AG-09/42) or subpocket III (Bürli-25 and AG-09/10). For AG-09/5, the nitro-substituted phenyl ring was located between subpockets II and III and coincided with the 5-membered imidazole ring of Frohn-11 within the template. Cilibrizzi-14x, AG-09/8, and AG-09/9 were overlaid in a three-pocket mode (Table 6).

## Discussion

FPRs have been implicated in the control of many inflammatory processes, promoting the recruitment and infiltration of phagocytes to sites of inflammation [reviewed in (Ye et al., 2009)], as well as resolving inflammation (Dufton and Perretti, 2010). However, the expression pattern of FPRs in non-phagocytic cells, especially that of FPR2, suggests that these receptors participate in functions other than innate immunity and may represent unique targets for therapeutic drug design. Because of the homology between GPCRs, it has been suggested and demonstrated that some of GPCR ligands thought previously to be “specific” may actually be recognized by unrelated GPCRs (Herold et al., 2003). Thus, screening heterologous GPCRs, in our case FPRs, with such ligands has the potential to identify novel agonist activity and potential leads for new therapeutics. Indeed, we screened a small library of 32 relatively low-molecular weight ligands (agonists and antagonists) of 24 different GPCRs and used SAR analysis to identify a number of novel and potent FPR agonists.

Screening of the GPCR ligands resulted in the discovery of CCK-1 receptor agonist A-71623 and bombesin-related BB<sub>1</sub>/BB<sub>2</sub> receptor antagonists PD168368 and PD176252 as FPR agonists. It should be noted that all three of these ligands contain Trp and an N-phenylurea moiety. Trp was also present in the structures of other compounds that we screened (e.g., somatostatin sst<sub>2</sub> receptor agonist L-054,264 and tachykinin NK<sub>1</sub> receptor antagonist L-732,138); however, both these ligands were inactive. Nevertheless, 3 of the 5 Trp-based GPCR ligands among all 32 compounds tested were FPR agonists. This represents a hit frequency of ~10%, which is much higher than that observed when screening a random collection of compound structures (~ 0.1%) (Edwards et al., 2005). Thus, the presence of both Trp and N-phenylurea aromatic fragments in the structure of peptide/peptoid GPCR ligands could be considered as a “risk factor” for cross-activity in relation to FPRs. Indeed, further screening of 97

PD176252/PD168368 analogs revealed 22 additional FPR agonists, some with very high potency and high efficacy.

Note that EC<sub>50</sub> values for the selected agonists in human neutrophils followed the same trend but were generally higher than those observed in FPR-transfected HL-60 cells. This is not surprising because of the differences in complexity between undifferentiated HL-60 cells and mature neutrophils [reviewed in (Birnie, 1988)]. Undifferentiated HL-60 cells lack many receptors, including endogenous FPR1 (Prossnitz et al., 1993), and other phagocyte functional responses, such as NADPH oxidase activity (Levy et al., 1990). In addition, Prossnitz *et al.* (Prossnitz et al., 1993) proposed that primary myeloid cells maintain a subpopulation of FPR in a low affinity, possibly G protein-free state, which is not a feature of FPR-transfected HL-60 cells. Thus, their work indicates that the environment where FPR are expressed plays an important role in the nature or amplitude of subsequent FPR-mediated responses, and confirmation of these responses in primary myeloid cells is essential. Clearly, further work is important to evaluate the role of cellular complexity, G protein availability, and levels of individual FPR expression in modulating the relative amplitude of FPR-mediated responses in transfected cell lines versus primary phagocytes.

Although CCK receptor agonists can modulate leukocyte functions, including activation of Ca<sup>2+</sup> mobilization in JURKAT T lymphocytic cells and monocyte chemotaxis (Sacerdote et al., 1988;Lignon et al., 1993;Carrasco et al., 1997), this is a first report that CCK-1 receptor agonist A-71623 can activate Ca<sup>2+</sup> mobilization in cells via FPRs. Agonistic activity of A-71623 in HL-60 cells transfected with FPR1/FPR2 can be related to the specific structure of this CCK-1 receptor agonist, which resembles structures of PD168368 and PD176252 [i.e., three aromatic fragments, including a Trp moiety, emerging from the same carbon atom in the  $\alpha$ -position (Figure 1A)].



To date, several BB<sub>1</sub>/BB<sub>2</sub> antagonists have been reported, including PD165929, PD168368, and PD176252 (Eden et al., 1996; Ryan et al., 1999). These compounds are known as peptoids, and represent non-peptide ligands that were designed based on the chemical structure of the mammalian neuropeptide (Horwell, 1995). PD168368 has high affinity for BB<sub>1</sub>, a 30- to 60-fold lower affinity for BB<sub>2</sub>, and a >300 fold lower affinity for BB<sub>3</sub> and BB<sub>4</sub> (Ryan et al., 1999), whereas PD176252 has nanomolar affinity for both BB<sub>1</sub> and BB<sub>2</sub> (Ashwood et al., 1998; Moody et al., 2003). On the other hand, cross-activity of these BB<sub>1</sub>/BB<sub>2</sub> antagonists for other GPCRs has not been reported. Given the potent effects of PD176252 and PD168368 at FPR1 and FPR2, our results indicate that these compounds are in fact not selective BB<sub>1</sub>/BB<sub>2</sub> ligands. Note, however, that all other BB<sub>1</sub>/BB<sub>2</sub> ligands tested were inactive, indicating that human neutrophils do not express functional BB<sub>1</sub>/BB<sub>2</sub> receptors, as has been suggested previously (Djanani and Kahler, 2002). Thus, our results show that FPR agonist activity is due to specific structural features of PD168368 and PD176252. Indeed, further SAR analysis of PD168368 and PD176252 analogs identified several additional FPR agonists with EC<sub>50</sub> values in the low nanomolar range, and these potent FPR agonists activated a number of phagocyte functional responses.

PD168368 and PD176252 have been used to study the role of BB<sub>1</sub>/BB<sub>2</sub> in physiological and pathological processes. For example, PD176252 inhibited the growth of lung cancer and head and neck squamous cell carcinoma cells, potentiated the growth inhibitory effects of histone deacetylase inhibitors, inhibited Ca<sup>2+</sup> flux in GRP/bombesin-stimulated lung cancer cells, and stimulated cell growth (Moody et al., 2000; Moody et al., 2006; Zhang et al., 2007a). Similarly, PD168368 inhibited NMB-stimulated cellular signaling and inhibited NMB-induced proliferation of rat C6 glioblastoma cells and NCI-H1299 lung cancer cells (Ryan et al., 1999; Moody et al., 2000). Here, we demonstrate that PD168368 and PD176252 and their

analogs can also activate a number of host defense functions in human and murine neutrophils. Thus, the effects of the BB<sub>1</sub>/BB<sub>2</sub> antagonists PD168368 and PD176252 on experimental animals or *in vitro/ex vivo* systems with a high content of phagocytic cells should be reevaluated to consider the potential innate immune enhancing effects of these compounds via FPR activation.

Pharmacophore modeling represents a rational approach for optimization of candidate small-molecule receptor ligands and screening for bioactive ligand conformations (Wolber et al., 2008). Through field point analysis of the relatively specific FPR2 agonists identified here, we were able to revise our previously published pharmacophore model of FPR2 agonists (Kirpotina et al., 2010). The revised model suggests the existence of three hydrophobic/aromatic subpockets and several binding poses of FPR2 agonists onto these subpockets. This is not surprising, as analysis of different agonists binding to the  $\beta_2$ -adrenergic receptor predicted different poses with various sets of optimal interaction inside of the local binding site (Katritch et al., 2009). Our pharmacophore model has similarities with the proposed interaction mode between the tetrapeptide WNleYM and FPR2 (Wan et al., 2007). However, because of the high flexibility of this peptide molecule, alignment of WNleYM conformations on our current FPR2 pharmacophore model could not be solved by the field point approach. Consequently, FPR2 agonists with three aromatic fragments linked to the same carbon atom in the  $\alpha$ -position may achieve an optimal binding arrangement and trigger more conformational changes within the FPR2 transmembrane region, as compared to the previously described dumbbell-shaped FPR2 agonists (see compounds used here for alignments on the template; Table 6).

Although our pharmacophore model represents a ligand-based view of the active site for FPR2, identification of the actual amino acid residues that comprise the ligand-binding site is complicated by the lack of crystallographic, site-directed mutagenesis, and cross-linking data. On the other hand, the similarity between GPCR ligands could reflect a similarity between their

binding sites (Gloriam et al., 2009). Thus, since amino acids (in particular Tyr-220) in transmembrane region 5 (TM-5) of the neuromedin receptor (BB<sub>1</sub>) play a major role in PD168368 binding (Tokita et al., 2001), it can be hypothesized that the binding site for PD168368, PD176252, and analogs may lie in the TM-5 region of FPR2. Indeed, the amino sequence <sup>201</sup>RGIIR<sup>205</sup> is conserved in TM-5 of most species variants for both FPR1 and FPR2 (Alvarez et al., 1996), and site-directed mutagenesis supports the role of residues Arg-201 and Arg-205 in positioning fMLF in the FPR1-binding pocket (Mills et al., 2000). Although bombesin-related receptors and FPRs are phylogenetically quite far from each other in the human *Rhodopsin* receptor family (Gloriam et al., 2009), it appears that conserved residues in these GPCRs results in ligand promiscuity among unrelated receptor targets.

In summary, we have identified a class of compounds, including bombesin BB<sub>1</sub>/BB<sub>2</sub> antagonists PD176252 and PD168368, which are potent FPR1 and FPR2 agonists. Indeed, AG-10/16 and AG-10/22 represent the most potent non-peptide FPR2 agonists reported to date. Thus, because of their potency and high efficacy, PD168368 and PD176252 and their analogs represent important leads for therapeutic development in regulating FPR function, and these compounds can serve as scaffolds for the development of novel, potent, and selective FPR2 agonists. On the other hand, the previously reported effects of these compounds that have been attributed solely to activity as BB<sub>1</sub>/BB<sub>2</sub> antagonists, such as effects on animal behavior (Merali et al., 2006) and cell proliferation (Moody et al., 2000; Moody et al., 2003) should also be reevaluated for contributions of FPR.

## Acknowledgements

We thank Dr. Marie-Josèphe Rabiet and Francois Boulet (CEA, DSV, iRTSV, Laboratoire Biochimie et Biophysique des Systèmes Intégrés, Grenoble, France) for kindly providing FPR-transfected HL-60 cells.

### **Authorship Contributions.**

*Participated in research design:* Schepetkin, Khlebnikov, Jutila, and Quinn.

*Conducted experiments:* Schepetkin, Kirpotina, and Khlebnikov.

*Performed data analysis:* Schepetkin, Kirpotina, Khlebnikov, and Quinn.

*Wrote or contributed to the writing of the manuscript:* Schepetkin, Khlebnikov, Jutila, and Quinn.

*Other:* Quinn and Jutila acquired funding for the research.

## References

- Alvarez V, Coto E, Setien F, Gonzalez-Roces S and Lopez-Larrea C (1996) Molecular Evolution of the N-Formyl Peptide and C5a Receptors in Non-Human Primates. *Immunogenetics* **44**:446-452.
- Ashwood V, Brownhill V, Higginbottom M, Horwell D C, Hughes J, Lewthwaite R A, McKnight A T, Pinnock R D, Pritchard M C, Suman-Chauhan N, Webb C and Williams S C (1998) PD176252--the First High Affinity Non-Peptide Gastrin-Releasing Peptide (BB2) Receptor Antagonist. *Bioorg Med Chem Lett* **8**:2589-2594.
- Bae YS, Lee H Y, Jo E J, Kim J I, Kang H K, Ye R D, Kwak J Y and Ryu S H (2004) Identification of Peptides That Antagonize Formyl Peptide Receptor-Like 1-Mediated Signaling. *J Immunol* **173**:607-614.
- Bae YS, Park J C, He R, Ye R D, Kwak J Y, Suh P G and Ho R S (2003a) Differential Signaling of Formyl Peptide Receptor-Like 1 by Trp-Lys-Tyr-Met-Val-Met-CONH<sub>2</sub> or Lipoxin A4 in Human Neutrophils. *Mol Pharmacol* **64**:721-730.
- Bae YS, Yi H J, Lee H Y, Jo E J, Kim J I, Lee T G, Ye R D, Kwak J Y and Ryu S H (2003b) Differential Activation of Formyl Peptide Receptor-Like 1 by Peptide Ligands. *J Immunol* **171**:6807-6813.
- Birnie GD (1988) The HL60 Cell Line: a Model System for Studying Human Myeloid Cell Differentiation. *Br J Cancer Suppl* **9**:41-45.
- Bürli RW, Xu H, Zou X, Muller K, Golden J, Frohn M, Adlam M, Plant M H, Wong M, McElvain M, Regal K, Viswanadhan V N, Tagari P and Hungate R (2006) Potent HFPRL1 (ALXR) Agonists As Potential Anti-Inflammatory Agents. *Bioorg Med Chem Lett* **16**:3713-3718.
- Carrasco M, Del R M, Hernanz A and De la Fuente M (1997) Inhibition of Human Neutrophil Functions by Sulfated and Nonsulfated Cholecystokinin Octapeptides. *Peptides* **18**:415-422.
- Cavicchioni G, Fraulini A, Falzarano S and Spisani S (2006) Structure-Activity Relationship of for-L-Met L-Leu-L-Phe-OMe Analogues in Human Neutrophils. *Bioorg Chem* **34**:298-318.
- Cheeseright T, Mackey M, Rose S and Vinter A (2006) Molecular Field Extrema As Descriptors of Biological Activity: Definition and Validation. *J Chem Inf Model* **46**:665-676.
- Cheeseright T, Mackey M, Rose S and Vinter A (2007) Molecular Field Technology Applied to Virtual Screening and Finding the Bioactive Conformation. *Expert Opin Drug Discov* **2**:131-144.
- Chen X, Yang D, Shen W, Dong H F, Wang J M, Oppenheim J J and Howard M Z (2000) Characterization of Chenodeoxycholic Acid As an Endogenous Antagonist of the G-Coupled Formyl Peptide Receptors. *Inflamm Res* **49**:744-755.
- Christophe T, Karlsson A, Rabiet M J, Boulay F and Dahlgren C (2002) Phagocyte Activation by Trp-Lys-Tyr-Met-Val-Met, Acting Through FPRL1/LXA<sub>4</sub>R, Is Not Affected by Lipoxin A<sub>4</sub>. *Scand J Immunol* **56**:470-476.

Cilibrizzi A, Quinn M T, Kirpotina L N, Schepetkin I A, Holderness J, Ye R D, Rabiet M J, Biancalani C, Cesari N, Graziano A, Vergelli C, Pieretti S, Dal P, V and Giovannoni M P (2009) 6-Methyl-2,4-Disubstituted Pyridazin-3(2H)-Ones: A Novel Class of Small-Molecule Agonists for Formyl Peptide Receptors. *J Med Chem* **52**:5054-5057.

Daiber A, August M, Baldus S, Wendt M, Oelze M, Sydow K, Kleschyov A L and Munzel T (2004) Measurement of NAD(P)H Oxidase-Derived Superoxide With the Luminol Analogue L-012. *Free Radic Biol Med* **36**:101-111.

Djanani AM and Kahler C (2002) Modulation of Inflammation by Vasoactive Intestinal Peptide and Bombesin: Lack of Effects on Neutrophil Apoptosis. *Acta Med Austriaca* **29**:93-96.

Dufton N and Perretti M (2010) Therapeutic Anti-Inflammatory Potential of Formyl-Peptide Receptor Agonists. *Pharmacol Ther* **127**:175-188.

Eden JM, Hall M D, Higginbottom M, Horwell D C, Howson W, Hughes J, Jordan R E, Lewthwaite R A, Martin K, McKnight A T, Otoole J C, Pinnock R D, Pritchard M C, SumanChauhan N and Williams S C (1996) PD165929 - The First High Affinity Non-Peptide Neuromedin-B (NMB) Receptor Selective Antagonist. *Bioorg Med Chem Lett* **6**:2617-2622.

Edwards BS, Bologa C, Young S M, Balakin K V, Prossnitz E R, Savchuck N P, Sklar L A and Oprea T I (2005) Integration of Virtual Screening With High-Throughput Flow Cytometry to Identify Novel Small Molecule Formylpeptide Receptor Antagonists. *Mol Pharmacol* **68**:1301-1310.

Fredriksson R, Lagerstrom M C, Lundin L G and Schioth H B (2003) The G-Protein-Coupled Receptors in the Human Genome Form Five Main Families. Phylogenetic Analysis, Paralogon Groups, and Fingerprints. *Mol Pharmacol* **63**:1256-1272.

Frohn M, Xu H, Zou X, Chang C, McElvaine M, Plant M H, Wong M, Tagari P, Hungate R and Bürli R W (2007) New 'Chemical Probes' to Examine the Role of the HFPRL1 (or ALXR) Receptor in Inflammation. *Bioorg Med Chem* **17**:6633-6637.

Gavins FN (2010) Are Formyl Peptide Receptors Novel Targets for Therapeutic Intervention in Ischaemia-Reperfusion Injury? *Trends Pharmacol Sci* **31**:266-276.

Gloriam DE, Foord S M, Blaney F E and Garland S L (2009) Definition of the G Protein-Coupled Receptor Transmembrane Bundle Binding Pocket and Calculation of Receptor Similarities for Drug Design. *J Med Chem* **52**:4429-4442.

Herold CL, Behm D J, Buckley P T, Foley J J, Wixted W E, Sarau H M and Douglas S A (2003) The Neuromedin B Receptor Antagonist, BIM-23127, Is a Potent Antagonist at Human and Rat Urotensin-II Receptors. *Br J Pharmacol* **139**:203-207.

Horwell DC (1995) The 'Peptoid' Approach to the Design of Non-Peptide, Small Molecule Agonists and Antagonists of Neuropeptides. *Trends Biotechnol* **13**:132-134.

Karlsson J, Fu H M, Boulay F, Bylund J and Dahlgren C (2006) The Peptide Trp-Lys-Tyr-Met-Val-D-Met Activates Neutrophils Through the Formyl Peptide Receptor Only When Signaling Through the Formylpeptide Receptor Like 1 Is Blocked - A Receptor Switch With Implications

for Signal Transduction Studies With Inhibitors and Receptor Antagonists. *Biochem Pharmacol* **71**:1488-1496.

Katritch V, Reynolds K A, Cherezov V, Hanson M A, Roth C B, Yeager M and Abagyan R (2009) Analysis of Full and Partial Agonists Binding to B<sub>2</sub>-Adrenergic Receptor Suggests a Role of Transmembrane Helix V in Agonist-Specific Conformational Changes. *J Mol Recognit* **22**:307-318.

Katritch V, Rueda M, Lam P C, Yeager M and Abagyan R (2010) GPCR 3D Homology Models for Ligand Screening: Lessons Learned From Blind Predictions of Adenosine A2a Receptor Complex. *Proteins* **78**:197-211.

Kawamata Y, Fujii R, Hosoya M, Harada M, Yoshida H, Miwa M, Fukusumi S, Habata Y, Itoh T, Shintani Y, Hinuma S, Fujisawa Y and Fujino M (2003) A G Protein-Coupled Receptor Responsive to Bile Acids. *J Biol Chem* **278**:9435-9440.

Kirpotina LN, Khlebnikov A I, Schepetkin I A, Ye R D, Rabiet M J, Jutila M A and Quinn M T (2010) Identification of Novel Small-Molecule Agonists for Human Formyl Peptide Receptors and Pharmacophore Models of Their Recognition. *Mol Pharmacol* **77**:159-170.

Kretschmer D, Gleske A K, Rautenberg M, Wang R, Koberle M, Bohn E, Schoneberg T, Rabiet M J, Boulay F, Klebanoff S J, van Kessel K A, Van Strijp J A, Otto M and Peschel A (2010) Human Formyl Peptide Receptor 2 Senses Highly Pathogenic *Staphylococcus Aureus*. *Cell Host Microbe* **7**:463-473.

Levy R, Rotrosen D, Nagauker O, Leto T L and Malech H L (1990) Induction of the Respiratory Burst in HL-60 Cells. Correlation of Function and Protein Expression. *J Immunol* **145**:2595-2601.

Liberles SD, Horowitz L F, Kuang D, Contos J J, Wilson K L, Siltberg-Liberles J, Liberles D A and Buck L B (2009) Formyl Peptide Receptors Are Candidate Chemosensory Receptors in the Vomeronasal Organ. *Proc Natl Acad Sci U S A* **106**:9842-9847.

Lignon MF, Bernad N and Martinez J (1993) Cholecystokinin Increases Intracellular Ca<sup>2+</sup> Concentration in the Human JURKAT T Lymphocyte Cell Line. *Eur J Pharmacol* **245**:241-246.

Merali Z, Bedard T, Andrews N, Davis B, McKnight A T, Gonzalez M I, Pritchard M, Kent P and Anisman H (2006) Bombesin Receptors As a Novel Anti-Anxiety Therapeutic Target: BB1 Receptor Actions on Anxiety Through Alterations of Serotonin Activity. *J Neurosci* **26**:10387-10396.

Mills JS, Miettinen H M, Cummings D and Jesaitis A J (2000) Characterization of the Binding Site on the Formyl Peptide Receptor Using Three Receptor Mutants and Analogs of Met-Leu-Phe and Met-Met-Trp-Leu-Leu. *J Biol Chem* **275**:39012-39017.

Moody TW, Jensen R T, Garcia L and Leyton J (2000) Nonpeptide Neuromedin B Receptor Antagonists Inhibit the Proliferation of C6 Cells. *Eur J Pharmacol* **409**:133-142.



- Moody TW, Leyton J, Garcia-Marin L and Jensen R T (2003) Nonpeptide Gastrin Releasing Peptide Receptor Antagonists Inhibit the Proliferation of Lung Cancer Cells. *Eur J Pharmacol* **474**:21-29.
- Moody TW, Nakagawa T, Kang Y, Jakowlew S, Chan D and Jensen R T (2006) Bombesin/Gastrin-Releasing Peptide Receptor Antagonists Increase the Ability of Histone Deacetylase Inhibitors to Reduce Lung Cancer Proliferation. *J Mol Neurosci* **28**:231-238.
- Movitz C, Brive L, Hellstrand K, Rabiet M J and Dahlgren C (2010) The Annexin I Sequence Gln(9)-Ala(10)-Trp(11)-Phe(12) Is a Core Structure for Interaction With the Formyl Peptide Receptor 1. *J Biol Chem* **285**:14338-14345.
- Nanamori M, Cheng X, Mei J, Sang H, Xuan Y, Zhou C, Wang M W and Ye R D (2004) A Novel Nonpeptide Ligand for Formyl Peptide Receptor-Like 1. *Mol Pharmacol* **66**:1213-1222.
- Parravicini C, Abbracchio M P, Fantucci P and Ranghino G (2010) Forced Unbinding of GPR17 Ligands From Wild Type and R255I Mutant Receptor Models Through a Computational Approach. *BMC Struct Biol* **10**:8.
- Prossnitz ER, Quehenberger O, Cochrane C G and Ye R D (1993) Signal Transducing Properties of the N-Formyl Peptide Receptor Expressed in Undifferentiated HL60 Cells. *J Immunol* **151**:5704-5715.
- Raoof M, Zhang Q, Itagaki K and Hauser C J (2010) Mitochondrial Peptides Are Potent Immune Activators That Activate Human Neutrophils Via FPR-1. *J Trauma* **68**:1328-1332.
- Ryan RR, Katsuno T, Mantey S A, Pradhan T K, Weber H C, Coy D H, Battey J F and Jensen R T (1999) Comparative Pharmacology of the Nonpeptide Neuromedin B Receptor Antagonist PD 168368. *J Pharmacol Exp Ther* **290**:1202-1211.
- Sacerdote P, Ruff M R and Pert C B (1988) Cholecystokinin and the Immune System: Receptor-Mediated Chemotaxis of Human and Rat Monocytes. *Peptides* **9 Suppl 1**:29-34.
- Schepetkin IA, Kirpotina L N, Khlebnikov A I and Quinn M T (2007) High-Throughput Screening for Small-Molecule Activators of Neutrophils: Identification of Novel N-Formyl Peptide Receptor Agonists. *Mol Pharmacol* **71**:1061-1074.
- Schepetkin IA, Kirpotina L N, Tian J, Khlebnikov A I, Ye R D and Quinn M T (2008) Identification of Novel Formyl Peptide Receptor-Like 1 Agonists That Induce Macrophage Tumor Necrosis Factor  $\alpha$  Production. *Mol Pharmacol* **74**:392-402.
- Schiffmann E, Corcoran B A and Wahl S M (1975) N-Formylmethionyl Peptides As Chemoattractants for Leucocytes. *Proc Natl Acad Sci USA* **72**:1059-1062.
- Sugg EE, Kimery M J, Ding J M, Kenakin D C, Miller L J, Queen K L and Rimele T J (1995) CCK-A Receptor Selective Antagonists Derived From the CCK-A Receptor Selective Tetrapeptide Agonist Boc-Trp-Lys(Tac)-Asp-MePhe-NH<sub>2</sub> (A-71623). *J Med Chem* **38**:207-211.

Thoren FB, Karlsson J, Dahlgren C and Forsman H (2010) The Anionic Amphiphile SDS Is an Antagonist for the Human Neutrophil Formyl Peptide Receptor 1. *Biochem Pharmacol* **80**:389-395.

Tokita K, Hocart S J, Katsuno T, Mantey S A, Coy D H and Jensen R T (2001) Tyrosine 220 in the 5th Transmembrane Domain of the Neuromedin B Receptor Is Critical for the High Selectivity of the Peptoid Antagonist PD168368. *J Biol Chem* **276**:495-504.

Vinter JG (1994) Extended Electron Distributions Applied to the Molecular Mechanics of Some Intermolecular Interactions. *J Comput Aided Mol Des* **8**:653-668.

Wan HX, Zhou C, Zhang Y, Sun M, Wang X, Yu H, Yang X, Ye R D, Shen J K and Wang M W (2007) Discovery of Trp-Nle-Tyr-Met As a Novel Agonist for Human Formyl Peptide Receptor-Like 1. *Biochem Pharmacol* **74**:317-326.

Wolber G, Seidel T, Bendix F and Langer T (2008) Molecule-Pharmacophore Superpositioning and Pattern Matching in Computational Drug Design. *Drug Discov Today* **13**:23-29.

Ye RD, Boulay F, Wang J M, Dahlgren C, Gerard C, Parmentier M, Serhan C N and Murphy P M (2009) International Union of Basic and Clinical Pharmacology. LXXIII. Nomenclature for the Formyl Peptide Receptor (FPR) Family. *Pharmacol Rev* **61**:119-161.

Zhang Q, Bhola N E, Lui V W, Siwak D R, Thomas S M, Gubish C T, Siegfried J M, Mills G B, Shin D and Grandis J R (2007a) Antitumor Mechanisms of Combined Gastrin-Releasing Peptide Receptor and Epidermal Growth Factor Receptor Targeting in Head and Neck Cancer. *Mol Cancer Ther* **6**:1414-1424.

Zhang XZ, Pare P D and Sandford A J (2007b) PMN Degranulation in Relation to CD63 Expression and Genetic Polymorphisms in Healthy Individuals and COPD Patients. *Int J Mol Med* **19**:817-822.

## Footnotes

This work was supported in part by the National Institutes of Health [Grant P20 RR-020185 and Contract HHSN266200400009C], an equipment grant from the M.J. Murdock Charitable Trust, and the Montana State University Agricultural Experimental Station.

## Figure Legends

**Figure 1.** Structure and activity of selected GPCR agonists. **Panel A.** Chemical structures of cholecystokinin-1 (CCK-1) receptor agonist A-71623 and bombesin-related receptor BB<sub>1</sub> and BB<sub>2</sub> antagonists PD176252 and PD168368. **Panel B.** Human neutrophils were treated with 300 nM PD176252 or PD168368, 20  $\mu$ M A-716235, 5 nM fMLF (positive control), or 1% DMSO (negative control), and Ca<sup>2+</sup> mobilization was monitored for the indicated times (arrow indicates when treatment was added). Arrow indicates time of treatment addition. **Panel C.** Human neutrophils were treated with the indicated concentrations of PD168368, PD176252, A-716235, and fMLF (all in  $\mu$ M), and MPO release determined, as described under Materials and Methods. The data are presented as mean $\pm$ S.D. of triplicate samples. In Panels **B** and **C**, the data are from one experiment that is representative of three independent experiments.

**Figure 2.** Stimulation of human neutrophil migration by selected compounds. Human neutrophil chemotaxis toward the indicated concentrations of AG-10/1 and AG-10/2 was determined, as described under Materials and Methods. The data are presented as the mean  $\pm$  S.D. of triplicate samples from one experiment that is representative of three independent experiments.

**Figure 3.** ROS production by human neutrophils treated with WKYMVm or AG-10/22. **Panel A:** Kinetic curves of ROS production induced by 100 nM WKYMVm or 100 nM AG-10/22. Arrow indicates time of treatment addition. **Panel B:** Integrated luminescence (120 sec) induced in human neutrophils plotted against the compound concentration. The data are presented as the mean  $\pm$  S.D. of triplicate samples. A representative experiment from three independent experiments is shown in both Panels.

**Figure 4.** Desensitization of  $\text{Ca}^{2+}$  mobilization in human neutrophils by selected FPR agonists. Human neutrophils were loaded with Fluo-4AM dye and pretreated with vehicle (DMSO), PD168368 (10  $\mu\text{M}$ ), AG-10/16 (100 nM), 5 nM fMLF (**Panel A**), 5 nM WKYMVM (**Panel B**), or 5 nM WKYMVM (**Panel C**), and  $\text{Ca}^{2+}$  mobilization was monitored. The same wells were then treated with one of peptides (in 5-nM concentrations) as indicated, and  $\text{Ca}^{2+}$  mobilization was monitored following this second treatment. In all Panels, the data are representative experiments from three independent experiments.

**Figure 5.** Multi-molecule template for FPR2 and alignments of two molecules on the template. **Panel A:** The multi-molecule template was created using the best conformations of the following 5 molecules: AG-10/5, AG-10/8, AG-10/17, PD168368, and Frohn-11. Field points are colored as follows: blue, electron-rich (negative); red, electron-deficient (positive); yellow, van der Waals attractive (steric); and orange, hydrophobic. **Panel B.** Alignments for Cilibrizzi-14x and AG-09/42 in the template represent examples of two different modes of ligand–receptor interaction with the three hypothetical receptor subpockets I, II, and III. Arrows indicate directions of alignments for AG-09/42 in subpockets I/II and for Cilibrizzi-14x in subpockets I/III. Negative field points (blue spheres A and B) correspond to the receptor’s positively charged regions (e.g., amino and hydroxyl groups in the active site that are capable of forming hydrogen bonds with electronegative atoms of the agonist). Positive field points (red sphere C) correspond to the receptor’s negatively charged regions or to hydrogen bond acceptors in the FPR2 active site. Spheres  $\text{H}_1$ ,  $\text{H}_2$ , and  $\text{H}_3$  correspond to hydrophobic centers. Substituents  $\text{R}_1$ ,  $\text{R}_2$ , and  $\text{R}_3$  may influence lipophilicity, molar refraction, and atomic charges for respective groups of particular FPR2 agonists. Dashed lines show correspondences between centers of the

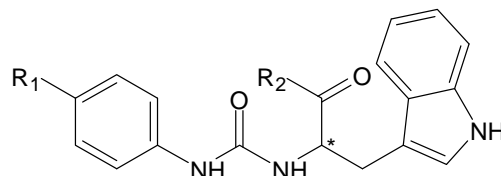
main field points on the multi-molecule template (Panel A) and their schematic representations in Panel B.

**Table 1.** Previously reported GPCR ligands that induced  $\text{Ca}^{2+}$  mobilization in human neutrophils and FPR-transfected HL-60 cells<sup>a</sup>

Compound	Previously Reported Activity for GPCR	$\text{Ca}^{2+}$ Mobilization, $\text{EC}_{50}$ ( $\mu\text{M}$ ) and Efficacy (%)			
		Neutrophils	FPR1	FPR2	FPR3
PD168368	$\text{BB}_1$ antagonist	$0.91 \pm 0.34$ (70)	$0.57 \pm 0.17$ (95)	$0.24 \pm 0.08$ (90)	$2.7 \pm 0.4$ (60)
PD176252	$\text{BB}_1/\text{BB}_2$ antagonist	$0.72 \pm 0.21$ (75)	$0.31 \pm 0.09$ (100)	$0.66 \pm 0.12$ (95)	NA
A-71623	CCK-1 receptor agonist	$18.3 \pm 3.1$ (55)	$18.0 \pm 3.8$ (50)	$16.4 \pm 3.1$ (85)	NA

<sup>a</sup> The  $\text{EC}_{50}$  values are presented as the mean  $\pm$  SD of three independent experiments, in which median effective concentration values ( $\text{EC}_{50}$ ) were determined by nonlinear regression analysis of the dose-response curves (5–6 points) generated using GraphPad Prism 5 with 95% confidential interval ( $p < 0.05$ ). Efficacy (in bracket) is expressed as percent of the response induced by 5 nM fMLF (FPR1) or 5 nM WKYMVm (FPR2 and FPR3).

**Table 2.** Trp-based derivatives that induced  $\text{Ca}^{2+}$  mobilization in human neutrophils and FPR-transfected HL-60 cells<sup>a</sup>

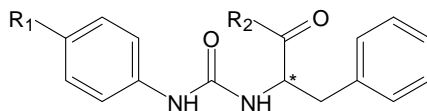


Compound	R <sub>1</sub>	R <sub>2</sub>	Enantiomer	Ca <sup>2+</sup> Mobilization, EC <sub>50</sub> (μM) and Efficacy (%)			
				Neutrophils	FPR1	FPR2	FPR3
AG-10/1	H		R/S	3.8 ± 0.5 (120)	2.7 ± 0.4 (100)	0.3 ± 0.07 (115)	13.5 ± 3.4 (60)
AG-10/2	Br		S	1.9 ± 0.5 (125)	0.5 ± 0.1 (120)	0.13 ± 0.03 (120)	7.6 ± 1.9 (85)
AG-10/3	Br		S	2.7 ± 0.6 (135)	2.2 ± 0.6 (120)	0.3 ± 0.06 (110)	2.4 ± 0.5 (80)

<sup>a</sup> See Table 1 legend. \*Location of the chiral center.



**Table 3.** Phe-based derivatives that induced  $\text{Ca}^{2+}$  mobilization in human neutrophils and FPR-transfected HL-60 cells<sup>a</sup>

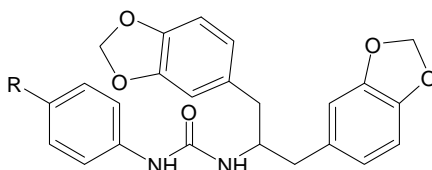


Compound	R <sub>1</sub>	R <sub>2</sub>	Enantiomer	Ca <sup>2+</sup> Mobilization, EC <sub>50</sub> (μM) and Efficacy (%)			
				Neutrophils	FPR1	FPR2	FPR3
AG-10/4	Br		S	3.2 ± 0.6 (115)	4.5 ± 1.1 (90)	0.14 ± 0.05 (100)	11.5 ± 2.8 (55)
AG-10/5	Br		S	1.2 ± 0.3 (140)	1.8 ± 0.5 (130)	0.04 ± 0.02 (115)	6.5 ± 1.7 (85)
AG-10/6	Cl		S	0.5 ± 0.2 (140)	2.9 ± 0.7 (100)	0.05 ± 0.01 (95)	3.1 ± 0.8 (65)
AG-10/7	S-CH <sub>3</sub>		S	6.6 ± 1.4 (50)	6.0 ± 1.4 (45)	0.3 ± 0.08 (75)	NA
AG-10/8	Br		S	0.7 ± 0.2 (145)	0.3 ± 0.08 (135)	0.004 ± 0.002 (115)	0.1 ± 0.03 (90)
AG-10/9	Br		S	0.5 ± 0.1 (110)	0.08 ± 0.02 (100)	0.007 ± 0.003 (100)	0.5 ± 0.1 (50)
AG-10/10	Br		S	4.4 ± 1.2 (85)	NA	0.16 ± 0.04 (85)	NA
AG-10/11	Br		R/S	9.7 ± 0.2 (90)	6.7 ± 1.6 (75)	0.25 ± 0.06 (55)	NA
AG-10/12	Cl		S	10.5 ± 2.6 (100)	4.2 ± 0.9 (85)	0.7 ± 0.3 (55)	NA
AG-10/13	CH <sub>2</sub> CH <sub>3</sub>		S	10.8 ± 2.2 (110)	3.1 ± 0.7 (105)	1.6 ± 0.3 (75)	NA

<sup>a</sup> See Table 1 legend. \*Location of the chiral center.

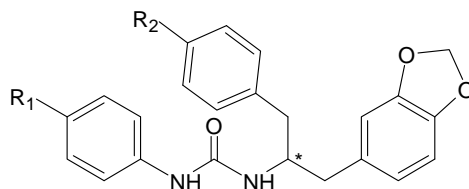
**Table 4.** Other analogs that induced  $\text{Ca}^{2+}$  mobilization in human neutrophils and FPR-transfected HL-60 cells<sup>a</sup>

**A.** N-[1,3-di(benzodioxolan-5-yl)propan-2-yl]-N'-phenylurea derivatives



Compound	R	$\text{Ca}^{2+}$ Mobilization, $\text{EC}_{50}$ ( $\mu\text{M}$ ) and Efficacy (%)			
		Neutrophils	FPR1	FPR2	FPR3
AG-10/14	H	$5.9 \pm 1.4$ (85)	NA	$0.006 \pm 0.002$ (95)	$3.3 \pm 0.7$ (45)
AG-10/15	F	$0.7 \pm 0.2$ (120)	$1.7 \pm 0.3$ (90)	$0.004 \pm 0.001$ (100)	$0.7 \pm 0.2$ (35)
AG-10/16	Cl	$0.06 \pm 0.02$ (150)	$3.7 \pm 0.8$ (110)	$0.002 \pm 0.0006$ (100)	$0.2 \pm 0.05$ (90)
AG-10/17	Br	$0.1 \pm 0.03$ (130)	$2.7 \pm 0.5$ (95)	$0.004 \pm 0.001$ (105)	$1.7 \pm 0.4$ (90)
AG-10/18	$\text{CH}_3$	$4.5 \pm 1.2$ (45)	$5.1 \pm 1.8$ (50)	$0.07 \pm 0.02$ (95)	$10.8 \pm 3.3$ (40)

**B.** N-[2-(1,3-benzodioxol-5-yl)-1-benzylethyl]-N'-phenylurea R/S derivatives



Compound	$\text{R}_1$	$\text{R}_2$	$\text{Ca}^{2+}$ Mobilization, $\text{EC}_{50}$ ( $\mu\text{M}$ ) and Efficacy (%)			
			Neutrophils	FPR1	FPR2	FPR3
AG-10/19	H	F	$1.2 \pm 0.3$ (115)	NA	$0.12 \pm 0.03$ (90)	$1.3 \pm 0.3$ (65)
AG-10/20	F	F	$0.14 \pm 0.03$ (150)	$7.5 \pm 1.6$ (70)	$0.02 \pm 0.005$ (105)	$1.2 \pm 0.3$ (75)
AG-10/21	$\text{CH}_3$	F	$10.1 \pm 2.4$ (80)	NA	$0.5 \pm 0.2$ (80)	NA
AG-10/22	Cl	O- $\text{CH}_3$	$0.013 \pm 0.003$ (140)	$0.11 \pm 0.03$ (130)	$0.0002 \pm 0.0001$ (130)	$0.05 \pm 0.02$ (115)

<sup>a</sup>See Table 1 legend. \*Location of the chiral center.

**Table 5.** Ca<sup>2+</sup> mobilization, chemotactic activity, and ROS production in neutrophils treated with selected agonists

Compound	Ca <sup>2+</sup> Mobilization in Murine Neutrophils (EC <sub>50</sub> , μM)	Chemotaxis (EC <sub>50</sub> , μM)		ROS Production in Human Neutrophils (EC <sub>50</sub> , μM)
		Human Neutrophils	Murine Neutrophils	
PD176252	0.2 ± 0.05 <sup>a</sup>	0.9 ± 0.3	8.3 ± 1.5	NA <sup>b</sup>
PD168368	0.1 ± 0.03	0.5 ± 0.15	2.1 ± 0.4	NA
AG-10/1 <sup>c</sup>	0.4 ± 0.1	0.004 ± 0.002	13.5 ± 4.2	0.43 ± 0.2
AG-10/2	0.4 ± 0.09	0.003 ± 0.001	3.4 ± 0.9	0.5 ± 0.2
AG-10/3	0.5 ± 0.2	0.022 ± 0.005	10.9 ± 2.1	8.0 ± 2.7
AG-10/4	3.5 ± 0.7	0.15 ± 0.04	10.8 ± 1.9	4.6 ± 1.3
AG-10/5	1.6 ± 0.4	0.09 ± 0.03	12.4 ± 2.2	4.5 ± 1.2
AG-10/6	1.2 ± 0.3	0.36 ± 0.1	1.2 ± 0.4	4.3 ± 1.3
AG-10/7	1.0 ± 0.3	0.68 ± 0.2	12.0 ± 2.6	9.3 ± 2.2
AG-10/8	0.08 ± 0.03	0.002 ± 0.001	0.96 ± 1.7	18.2 ± 4.3
AG-10/9	0.3 ± 0.07	0.02 ± 0.005	0.056 ± 0.022	1.9 ± 0.4
AG-10/10	0.2 ± 0.06	0.5 ± 0.2	0.005 ± 0.002	4.2 ± 0.9
AG-10/14	10.7 ± 1.9	0.65 ± 0.2	9.1 ± 1.7	1.4 ± 0.4
AG-10/15	0.1 ± 0.04	0.04 ± 0.01	1.6 ± 0.3	0.7 ± 0.16
AG-10/16	0.03 ± 0.01	0.18 ± 0.05	1.1 ± 0.2	1.1 ± 0.3
AG-10/17	0.06 ± 0.02	0.04 ± 0.01	0.56 ± 0.12	0.35 ± 0.08
AG-10/18	4.6 ± 0.9	2.1 ± 0.5	7.1 ± 1.3	NA
AG-10/19	0.9 ± 0.3	0.90 ± 0.3	19.0 ± 4.3	2.4 ± 0.6
AG-10/20	8.5 ± 1.9	0.04 ± 0.01	5.8 ± 1.7	0.8 ± 0.18
AG-10/21	4.5 ± 1.4	4.3 ± 1.1	29.3 ± 6.2	1.6 ± 0.4
AG-10/22	0.003 ± 0.001	0.006 ± 0.002	0.18 ± 0.07	0.23 ± 0.6
WKYMVm	0.01 ± 0.005	0.002 ± 0.001	1.6 ± 0.4	4.1 ± 0.9
WKYMVM	0.03 ± 0.01	0.04 ± 0.01	3.5 ± 1.2	125 ± 24.5
fMLF	0.14 ± 0.03	0.0005 ± 0.0002	14.6 ± 2.7	0.04 ± 0.02

<sup>a</sup>The data are presented as the mean ± SD of three independent experiments with cells from different donors or mice, in which median effective concentration values (EC<sub>50</sub>) were determined by nonlinear regression analysis of the dose–response curves (5–6 points) generated using GraphPad Prism 5 with 95% confidential interval ( $p < 0.05$ ).

<sup>b</sup>NA, non-active compound, if cell activation was <30% of control level over a concentration range of 0 to 40 μM.

<sup>c</sup>Compound formulas: AG-10/1, [(R/S) 3-(1H-indol-3-yl)-N-(4-methoxyphenyl)-2-(3-phenylureido)propanamide]; AG-10/2, [(S)-ethyl 1-(2-(3-(4-bromophenyl)ureido)-3-(1H-indol-3-yl)propanoyl)piperidine-4-carboxylate]; AG-10/3, [(S)-4-(2-(3-(4-bromophenyl)ureido)-3-(1H-indol-3-yl)propanoyl)-N-ethyl-2-methylpiperazine-1-carboxamide]; AG-10/4, [(S)-1-(4-bromophenyl)-3-(1-

oxo-3-phenyl-1-(pyrrolidin-1-yl)propan-2-yl)urea]; AG-10/5, [(S)-1-(4-bromophenyl)-3-(1-oxo-3-phenyl-1-(piperidin-1-yl)propan-2-yl)urea]; AG-10/6, [(S)-1-(4-chlorophenyl)-3-(1-oxo-3-phenyl-1-(piperidin-1-yl)propan-2-yl)urea]; AG-10/7, [(S)-1-(4-(methylthio)phenyl)-3-(1-oxo-3-phenyl-1-(piperidin-1-yl)propan-2-yl)urea]; AG-10/8, [(S)-2-(3-(4-bromophenyl)ureido)-N-(2-oxoazepan-3-yl)-3-phenylpropanamide]; AG-10/9, [(S)-ethyl 1-(2-(3-(4-bromophenyl)ureido)-3-phenylpropanoyl)piperidine-3-carboxylate]; AG-10/10, [(S)-ethyl 1-(2-(3-(4-bromophenyl)ureido)-3-phenylpropanoyl)piperidine-4-carboxylate]; AG-10/14, [N-[2-(1,3-benzodioxol-5-yl)-1-(1,3-benzodioxol-5-ylmethyl)ethyl]-N'-phenylurea]; AG-10/15, [N-[2-(1,3-benzodioxol-5-yl)-1-(1,3-benzodioxol-5-ylmethyl)ethyl]-N'-(4-fluorophenyl)urea]; AG-10/16, [N-[2-(1,3-benzodioxol-5-yl)-1-(1,3-benzodioxol-5-ylmethyl)ethyl]-N'-(4-chlorophenyl)urea]; AG-10/17, [N-[2-(1,3-benzodioxol-5-yl)-1-(1,3-benzodioxol-5-ylmethyl)ethyl]-N'-(4-bromophenyl)urea]; AG-10/20, [(R/S) N-[2-(1,3-benzodioxol-5-yl)-1-(4-fluorobenzyl)ethyl]-N'-(4-fluorophenyl)urea]; AG-10/22, [(R/S) N-[2-(1,3-benzodioxol-5-yl)-1-(4-methoxybenzyl)ethyl]-N'-(4-chlorophenyl)urea].

**Table 6.** Location in hypothetical hydrophobic subpockets of substituents from representative conformations obtained for the 5-molecule FPR2 template and alignments on this template of previously reported FPR agonists

	Compound	Subpocket I	Subpocket II	Subpocket III
Template	AG-10/8	4-bromophenyl	benzyl	2-oxazepan-3-yl
	PD168368	4-nitrophenyl	3-indolyl	1-(2-pyridyl)-1-cyclohexyl
	Frohn-11	5-methoxy-indole	benzimidazol-1-yl	ethyl
	AG-10/5	4-bromophenyl	benzyl	1-piperidyl
	AG-10/17	4-bromophenyl	1,3-benzodioxol-5-yl	1,3-benzodioxol-5-yl
Alignment	Cilibrizzi-14x	4-bromophenyl	methyl	4-methoxybenzyl
	Bürli-25	4-bromophenyl	methyl oriented to subpocket II	phenyl
	AG-09/3	4-bromophenyl	4-fluorophenyl	-
	AG-09/4	4-bromophenyl	3-chlorophenyl	-
	AG-09/5	4-chlorophenyl	2-nitrophenyl located between subpockets II and III; nitro group oriented to subpocket II	
	AG-09/6	4-methoxyphenyl	2-thienyl	-
	AG-09/8	4-nitrophenyl	fused benzene ring	4-methoxyphenyl
	AG-09/9	4-methoxyphenyl	thiazolidin-4-one-3-yl	fused benzene ring
	AG-09/10	4-methoxyphenyl	-	1-piperidyl
	AG-09/42	4-bromophenyl	4-methoxyphenyl	-

Figure 1

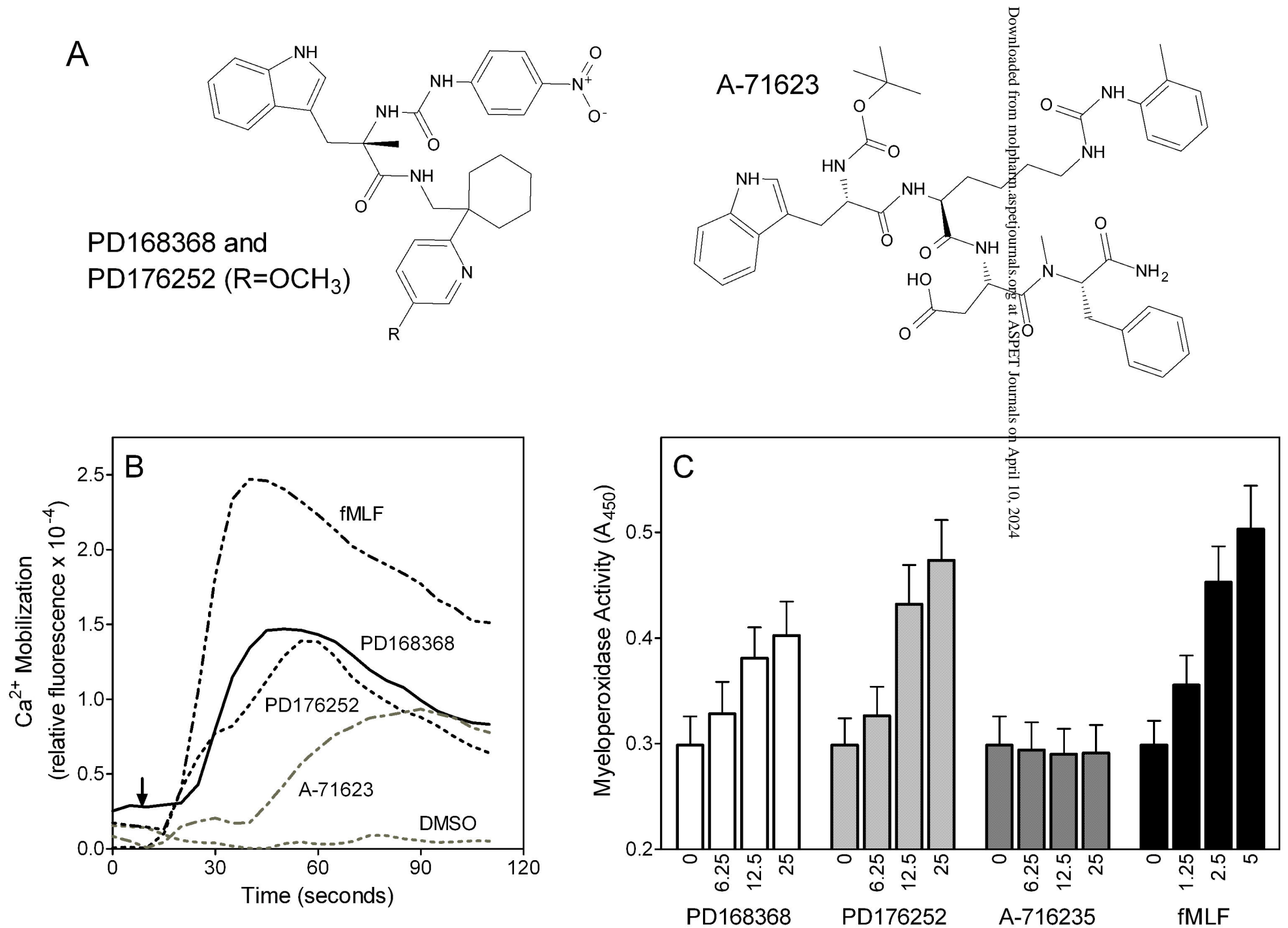


Figure 2

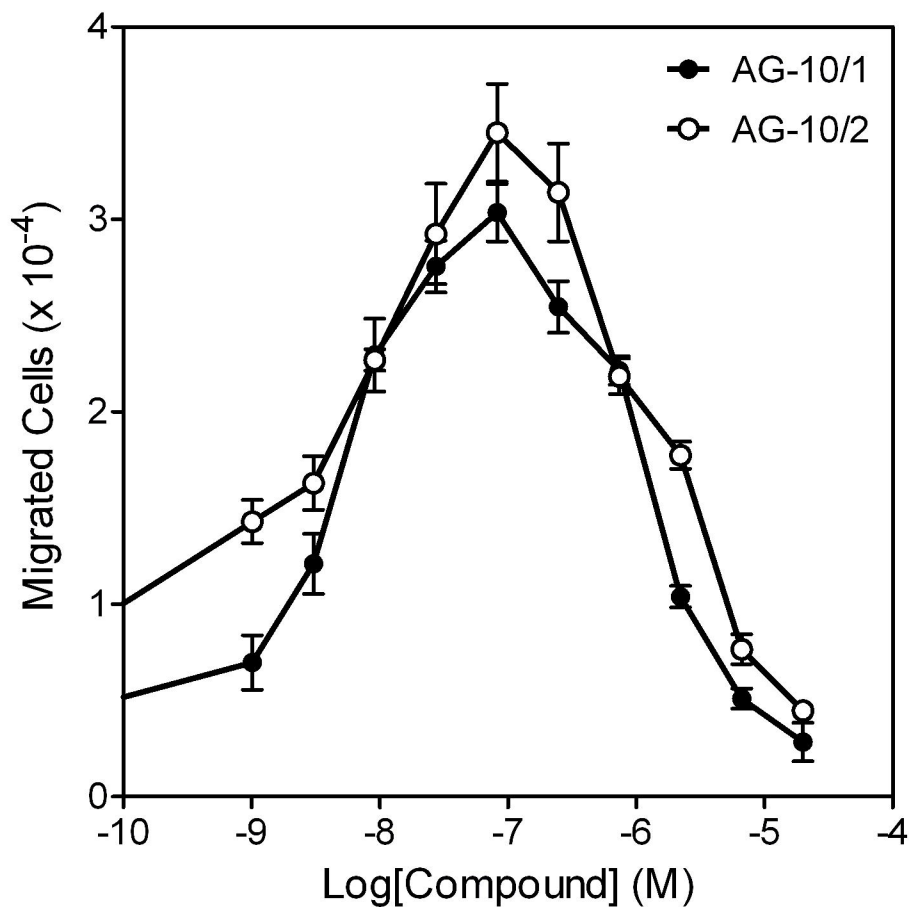


Figure 3

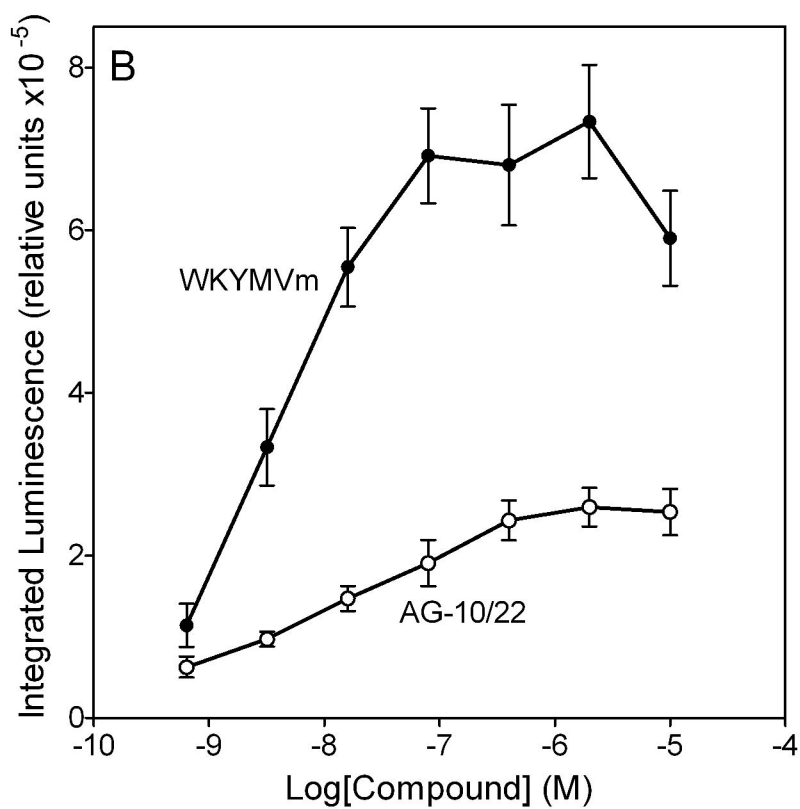
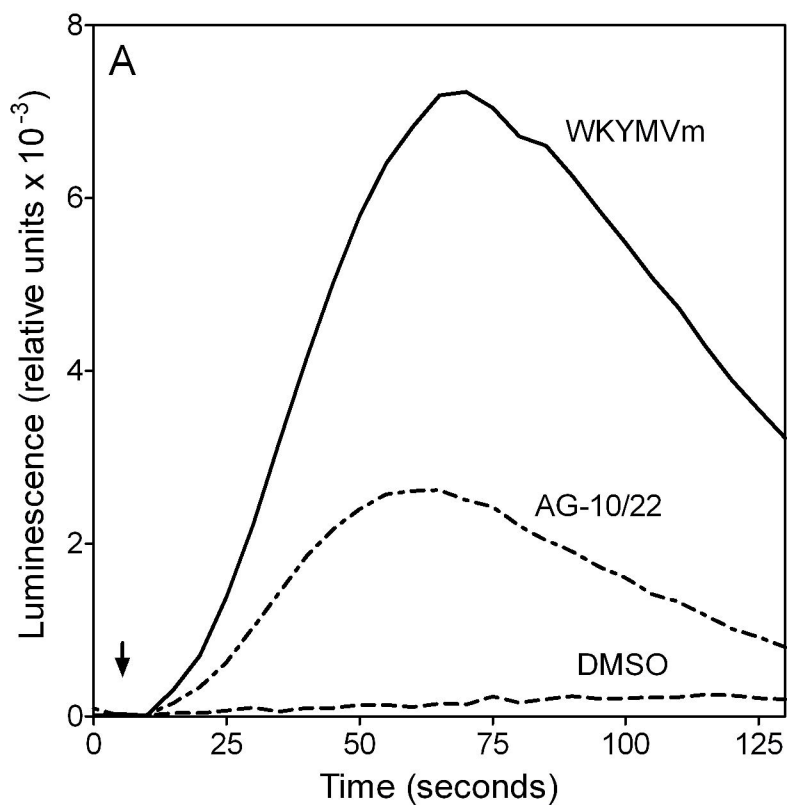




Figure 4

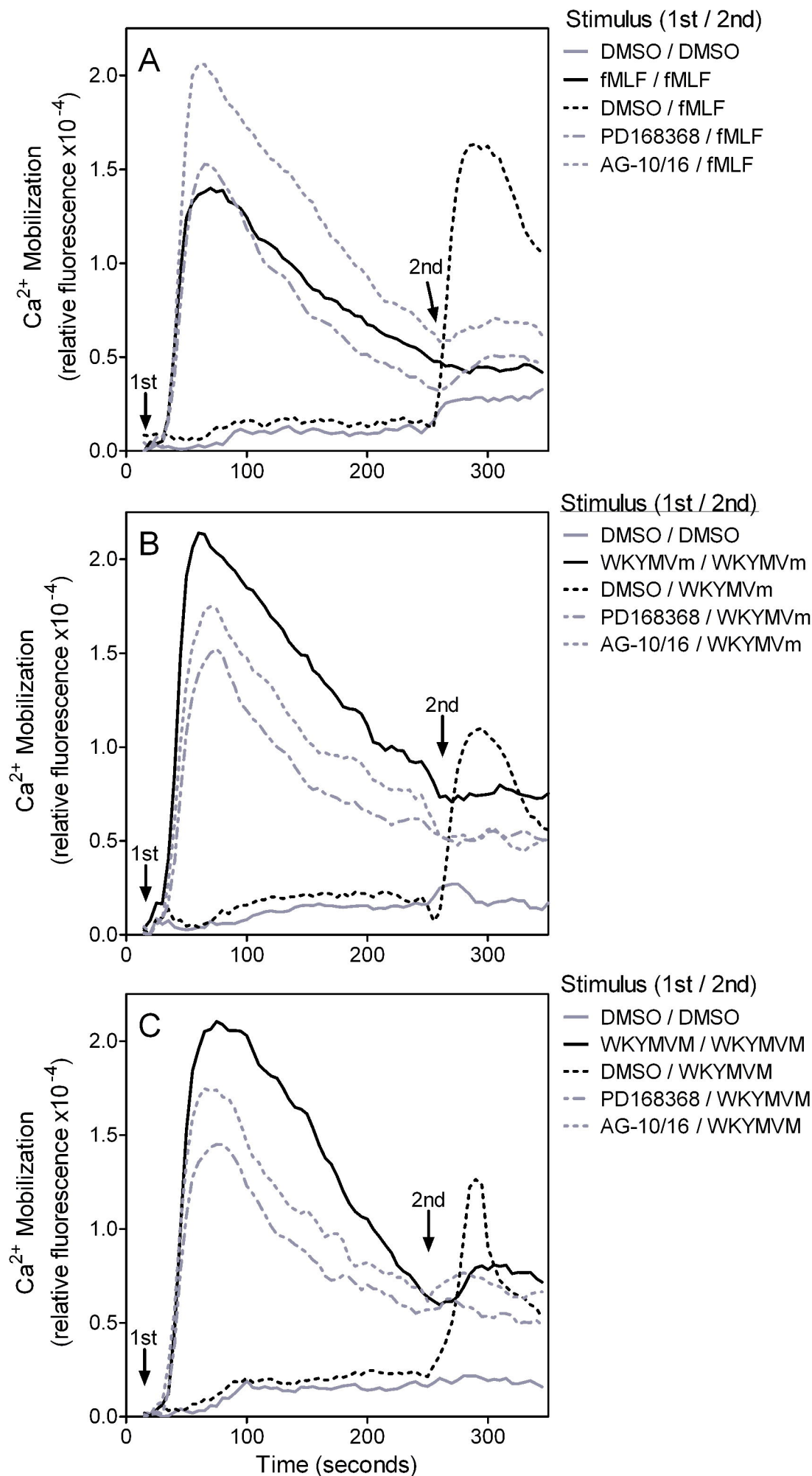


Figure 5

